

# An evolutionarily conserved gene family encodes proton-selective ion channels

Yu-Hsiang Tu,<sup>1</sup> Alexander J. Cooper,<sup>1\*†</sup> Bochuan Teng,<sup>1\*‡</sup> Rui B. Chang,<sup>1\*‡</sup> Daniel J. Artiga,<sup>1</sup> Heather N. Turner,<sup>1</sup> Eric M. Mulhall,<sup>1§</sup> Wenlei Ye,<sup>1||</sup> Andrew D. Smith,<sup>2</sup> Emily R. Liman<sup>1,3#</sup>

Ion channels form the basis for cellular electrical signaling. Despite the scores of genetically identified ion channels selective for other monatomic ions, only one type of proton-selective ion channel has been found in eukaryotic cells. By comparative transcriptome analysis of mouse taste receptor cells, we identified Otopetrin1 (OTOP1), a protein required for development of gravity-sensing otoconia in the vestibular system, as forming a proton-selective ion channel. We found that murine OTOP1 is enriched in acid-detecting taste receptor cells and is required for their zinc-sensitive proton conductance. Two related murine genes, *Otop2* and *Otop3*, and a *Drosophila* ortholog also encode proton channels. Evolutionary conservation of the gene family and its widespread tissue distribution suggest a broad role for proton channels in physiology and pathophysiology.

Ion channels include a large and diverse group of membrane proteins that rapidly, and with great selectivity, move ions across the cell membrane, performing crucial roles in cell signaling and homeostasis (1). Ion channels selective for each of the physiologically relevant ions, Na<sup>+</sup>, K<sup>+</sup>, Ca<sup>2+</sup>, and Cl<sup>-</sup>, have been described at the molecular and structural levels (2, 3), but only a few types of proton-selective ion channels (proton channels) have been described (4). One is the 96-amino acid M2 protein of influenza A, which conducts protons into the virion interior,

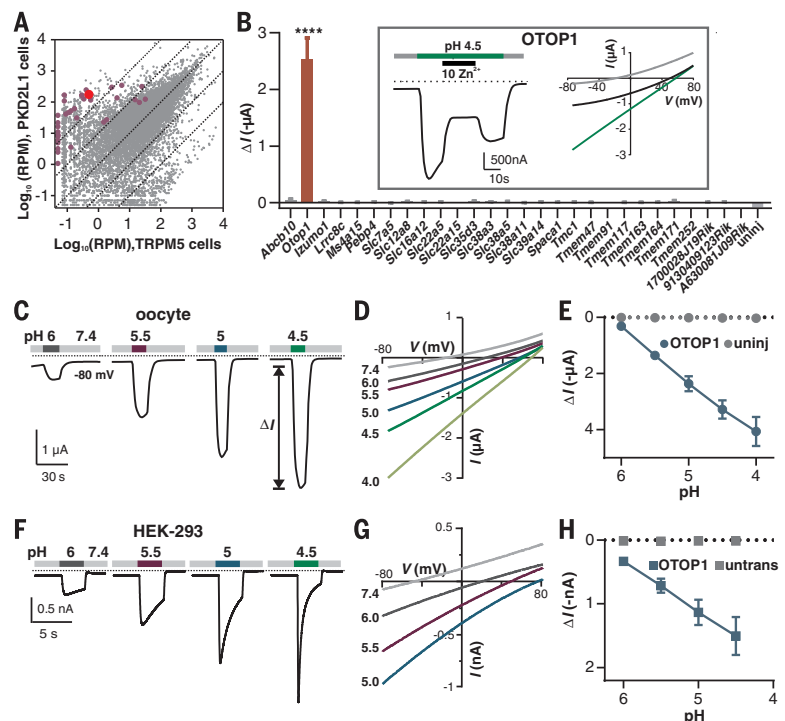
an essential step in the replication of the virus (5). The only proton-selective ion channel identified in eukaryotes is the voltage-gated Hv1 (6–8), which is present in immune cells, where it extrudes protons into the phagosome to inactivate infectious agents (9). Functional evidence indicates that ion channels that selectively transport protons into eukaryotic cells must also exist. For example, in acid-sensing taste receptor cells (TRCs), an inward-conducting Zn<sup>2+</sup>-sensitive proton current that is biophysically distinct from currents carried by Hv1 has been described (10, 11).

To identify candidates encoding such a proton channel, we compared the transcriptome of mouse TRCs positive for the inward-conducting Zn<sup>2+</sup>-sensitive proton current (PKD2L1 cells) with that of TRCs that lack the current (TRPM5 cells; Fig. 1A). We selected genes that were enriched in PKD2L1 cells and that encoded poorly characterized or uncharacterized transmembrane proteins (Fig. 1A and table S1) (see methods). We expressed the candidates in human embryonic kidney 293 (HEK-293) cells or *Xenopus* oocytes and measured ionic currents in response to lowering the extracellular pH (pH<sub>o</sub>) in the absence of extracellular Na<sup>+</sup>. Of the 41 cDNAs tested, only Otopetrin1 (*Otop1*), which encodes a protein (OTOP1) with 12 predicted transmembrane domains (12), generated large Zn<sup>2+</sup>-sensitive inward currents in response to extracellular acidification (Fig. 1B).

We characterized functional properties of OTOP1 expressed in *Xenopus* oocytes. Unless otherwise noted, the extracellular solution used in recordings

## Fig. 1. Expression analysis of taste-cell-enriched genes identifies OTOP1 as a previously unknown proton channel.

(A) Transcriptome profiling of PKD2L1 and TRPM5 taste receptor cells (each data point represents the average of five replicates). Genes tested by electrophysiology are highlighted in magenta or red (*Otop1*). RPM, reads per million. (B) Magnitude of currents evoked in response to pH 4.5 Na<sup>+</sup>-free solution in *Xenopus* oocytes expressing the genes indicated ( $V_m = -80$  mV; data are mean  $\pm$  SEM,  $n = 3$  to 37 cells; for OTOP1,  $n = 5$ ). \*\*\*\* $P < 0.0001$  compared to uninjected oocytes ( $n = 3$ ). One-way analysis of variance with Bonferroni correction. (Inset) Currents evoked in an OTOP1-expressing oocyte in response to the acid stimulus at  $V_m = -80$  mV (left) and the current-voltage ( $I$ - $V$ ) relationship before application (gray), during acid application (green), and during Zn<sup>2+</sup> application (black). (C) Current measured by two-electrode voltage clamp in a *Xenopus* oocyte expressing OTOP1 in response to Na<sup>+</sup>-free extracellular solutions with pH<sub>o</sub> as indicated ( $V_m = -80$  mV). (D)  $I$ - $V$  relation of the current in (A) from voltage ramps (1 V/s). (E) Evoked current ( $\Delta I$ ; mean  $\pm$  SEM) as a function of pH in *Xenopus* oocytes expressing OTOP1 (blue circle;  $n = 4$ ) and uninjected oocytes (gray circles;  $n = 4$ ). (F) Currents measured by whole-cell patch clamp recording in a HEK-293 cell expressing OTOP1 in Na<sup>+</sup>-free extracellular solutions (pH<sub>o</sub> = 7.3,  $V_m = -80$  mV). (G)  $I$ - $V$  relation of currents in an OTOP1-expressing HEK-293 cell from experiments as in (F) with voltage ramps (1 V/s). (H) Evoked currents ( $\Delta I$ ; mean  $\pm$  SEM) as a function of pH in HEK-293 cells expressing OTOP1 (blue squares;  $n = 5$ ) and untransfected cells (gray squares;  $n = 3$ ).



<sup>1</sup>Department of Biological Sciences, Section of Neurobiology, University of Southern California, Los Angeles, CA 90089, USA. <sup>2</sup>Department of Biological Sciences, Section of Molecular and Computational Biology, University of Southern California, Los Angeles, CA 90089, USA. <sup>3</sup>Bridge Institute, University of Southern California, Los Angeles, CA 90089, USA.

\*These authors contributed equally to this work. †Present address: Zilkha Neurogenetic Institute, Department of Cell and Neurobiology, Keck School of Medicine, University of Southern California, Los Angeles, CA 90089, USA. ‡Present address: Department of Neuroscience and Department of Cellular and Molecular Physiology, Yale University School of Medicine, New Haven, CT 06520, USA. §Present address: Department of Neurobiology, Harvard Medical School, Boston, MA 20115, USA. ||Present address: Department of Physiology, University of California, San Francisco, CA 94158, USA.

#Corresponding author. Email: liman@usc.edu

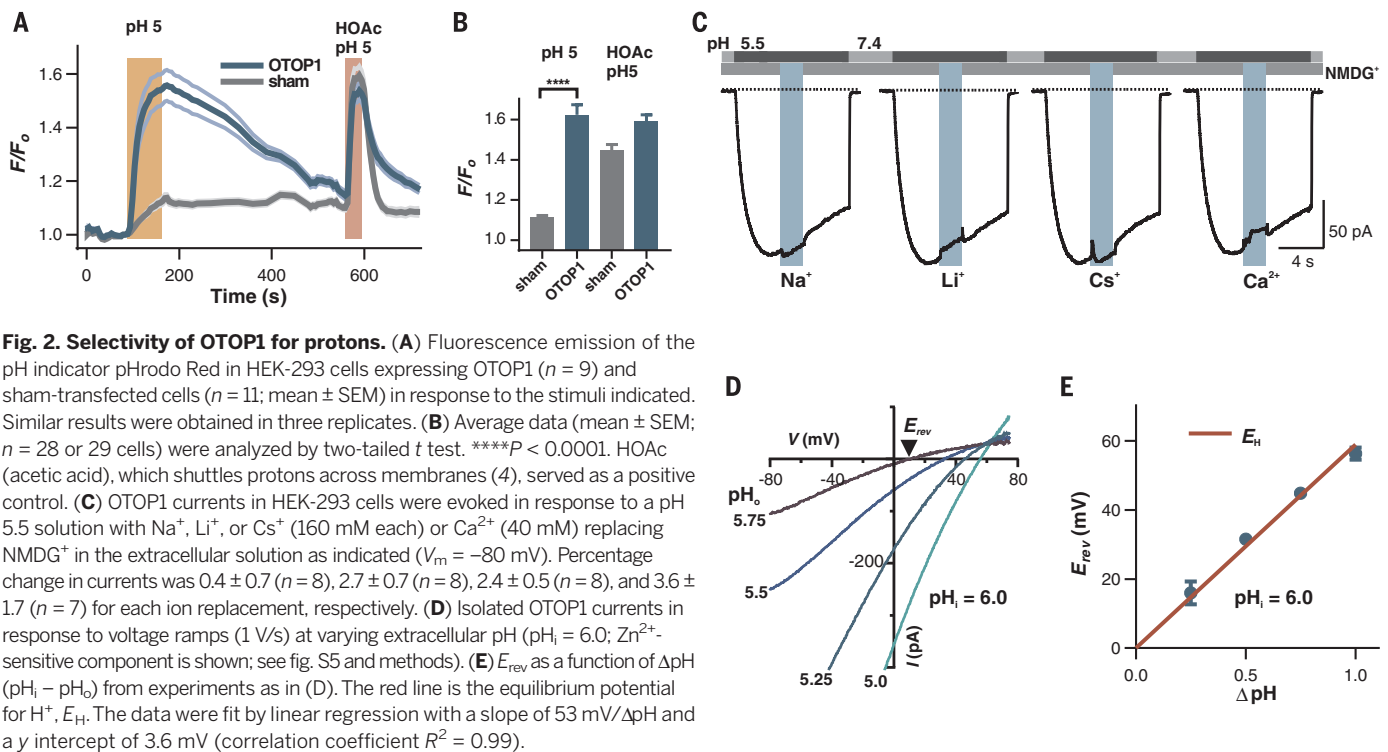


**Fig. 2. Selectivity of OTOPI for protons.** (A) Fluorescence emission of the pH indicator pHRodo Red in HEK-293 cells expressing OTOPI ( $n = 9$ ) and sham-transfected cells ( $n = 11$ ; mean  $\pm$  SEM) in response to the stimuli indicated. Similar results were obtained in three replicates. (B) Average data (mean  $\pm$  SEM;  $n = 28$  or 29 cells) were analyzed by two-tailed  $t$  test. \*\*\*\* $P < 0.0001$ . HOAc (acetic acid), which shuttles protons across membranes (4), served as a positive control. (C) OTOPI currents in HEK-293 cells were evoked in response to a pH 5.5 solution with  $\text{Na}^+$ ,  $\text{Li}^+$ , or  $\text{Cs}^+$  (160 mM each) or  $\text{Ca}^{2+}$  (40 mM) replacing  $\text{NMDG}^+$  in the extracellular solution as indicated ( $V_m = -80$  mV). Percentage change in currents was  $0.4 \pm 0.7$  ( $n = 8$ ),  $2.7 \pm 0.7$  ( $n = 8$ ),  $2.4 \pm 0.5$  ( $n = 8$ ), and  $3.6 \pm 1.7$  ( $n = 7$ ) for each ion replacement, respectively. (D) Isolated OTOPI currents in response to voltage ramps (1 V/s) at varying extracellular pH ( $\text{pH}_i = 6.0$ ;  $\text{Zn}^{2+}$ -sensitive component is shown; see fig. S5 and methods). (E)  $E_{\text{rev}}$  as a function of  $\Delta\text{pH}$  ( $\text{pH}_i - \text{pH}_o$ ) from experiments as in (D). The red line is the equilibrium potential for  $\text{H}^+$ ,  $E_{\text{H}}$ . The data were fit by linear regression with a slope of 53 mV/ $\Delta\text{pH}$  and a y intercept of 3.6 mV (correlation coefficient  $R^2 = 0.99$ ).

was  $\text{Na}^+$ -free [*N*-methyl-D-glucamine ( $\text{NMDG}^+$ )-based]. OTOPI currents increased monotonically as  $\text{pH}_o$  was lowered (Fig. 1, C to E) and the reversal potential ( $E_{\text{rev}}$ ) shifted toward more positive voltages (Fig. 1D and fig. S1A). The currents showed a small time-dependent change in amplitude in response to hyperpolarizing voltage steps, indicating that gating of OTOPI is mildly voltage-sensitive (fig. S1, B and C).

OTOPI also generated an ionic current in HEK-293 cells (Fig. 1, F to H). An N-terminal YFP (yellow fluorescent protein)-tagged protein confirmed the presence of OTOPI at the cell surface (fig. S2A). Lowering  $\text{pH}_o$  elicited large inward currents in OTOPI-expressing cells and, as in oocytes, the current magnitude increased monotonically with  $\text{pH}_o$  (Fig. 1, F to H). OTOPI currents in HEK-293 cells decayed within seconds, with faster kinetics observed in response to more acidic stimuli (Fig. 1F). The decay of the currents is likely to be due, in part, to a reduction in the driving force as protons accumulate in the cytosol. For a 15- $\mu\text{m}$ -diameter cell (1767 fL volume), a  $\text{H}^+$  current of 1000 pA flowing for 1 s will increase the total (bound + free) intracellular concentration of  $\text{H}^+$  by  $\sim 6$  mM (4). We confirmed that OTOPI mediated flux of protons into the cell cytosol with the membrane-permeant pH indicator pHRodo Red. In *Otop1*-transfected cells, but not in mock-transfected cells, lowering extracellular pH from 7.4 to 5.0 caused a large increase in emission of pHRodo Red (Fig. 2, A and B), corresponding to a large change in intracellular pH (fig. S2, B and C).

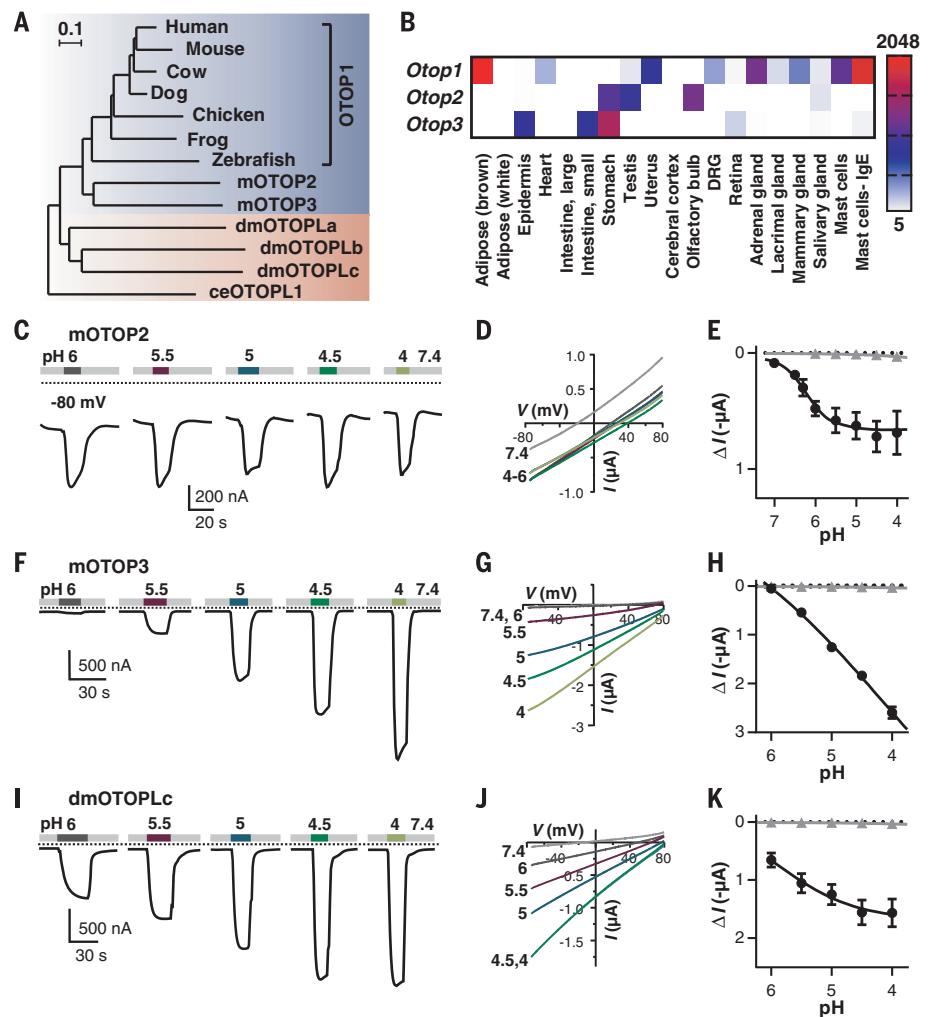
Hv1 and M2 are highly selective for protons, present in high nanomolar concentrations, over other cations whose concentrations are a million

times higher (4, 13). To determine if OTOPI is similarly proton-selective, we evoked *Otop1* currents by lowering  $\text{pH}_o$  from 7.4 to 5.5 and measured the effect of exchanging  $\text{NMDG}^+$  in the extracellular solution for equimolar concentrations of  $\text{Na}^+$ ,  $\text{Cs}^+$ , or  $\text{Li}^+$  or isosmotic concentrations of  $\text{Ca}^{2+}$  (Fig. 2C). In all cases, the observed change in current magnitude was less than 4%, indicating that OTOPI is not appreciably permeable to these ions. Similar experiments showed that OTOPI is not appreciably permeable to  $\text{K}^+$  (fig. S3). To directly assess the selectivity of the channel for protons, we measured the potential at which the current reversed direction, the reversal potential ( $E_{\text{rev}}$ ), as a function of the  $\text{H}^+$  gradient ( $\Delta\text{pH} = \text{pH}_i - \text{pH}_o$ ). To study a predominantly OTOPI current, we applied  $\text{Zn}^{2+}$  at a concentration that selectively and fully blocked the OTOPI current in HEK-293 cells and focused on the  $\text{Zn}^{2+}$ -sensitive component of the current (figs. S4 and S5, A and B). We limited  $\text{H}^+$  accumulation by setting  $\text{pH}_i$  at 6.0 and holding the membrane potential at  $E_{\text{rev}}$  (fig. S5A; see methods). Under these conditions,  $E_{\text{rev}}$  closely followed the Nernst prediction for an  $\text{H}^+$ -selective ion channel (Fig. 2, D and E). To determine the selectivity of OTOPI for  $\text{H}^+$  relative to  $\text{Na}^+$  and  $\text{Cl}^-$ , we measured  $E_{\text{rev}}$  upon replacement of  $\text{NMDG}^+$  by  $\text{Na}^+$  and with high and low concentrations of  $\text{Cl}^-$  in the extracellular solution. In no case did we observe any change in  $E_{\text{rev}}$  (fig. S5C). Assuming a change in  $E_{\text{rev}}$  of less than 5 mV, which would have been detectable, we used the Goldman-Hodgkin-Katz equation to calculate the selectivity of OTOPI for  $\text{H}^+$  relative to  $\text{Na}^+$  at greater than  $2 \times 10^5$ -fold and  $\text{H}^+$  to  $\text{Cl}^-$  at greater than  $1 \times 10^5$ -fold (13).

OTOPI is a member of the *otopetrin* family of proteins, which is evolutionarily conserved from nematodes to humans (12, 14) (Fig. 3A). We confirmed that human OTOPI (hOTOPI) forms a channel with properties similar to those of murine OTOPI (fig. S6). Murine OTOPI and OTOPI3 share 30 to 34% amino acid identity with murine OTOPI (fig. S7). Each shows a distinctive pattern of expression. *Otop1* is expressed in vestibular and taste cells, brown adipose tissue (15), heart, uterus, dorsal root ganglion, adrenal gland, mammary gland, and stimulated mast cells, whereas *Otop2* expression is highest in stomach, testis, and olfactory bulb, and *Otop3* is expressed in epidermis, small intestine, stomach, and retina [Fig. 3B; (16)]. When expressed in *Xenopus* oocytes, OTOPI2 and OTOPI3 both generated large currents in response to lowering  $\text{pH}_o$  in a  $\text{Na}^+$ -free solution. Compared with OTOPI and OTOPI3, OTOPI2 currents behaved anomalously; currents saturated at  $\sim\text{pH}$  5, and  $E_{\text{rev}}$  shifted little over a range of pH 4 to 6 (Fig. 3, C to E, and fig. S8A). OTOPI2 currents measured in HEK-293 cells had similar properties (fig. S9). Like OTOPI, OTOPI3 showed evidence of selectivity for  $\text{H}^+$ ; the magnitude of OTOPI3 currents increased linearly as a function of  $\text{pH}_o$  over the entire pH range tested (Fig. 3, F to H), and  $E_{\text{rev}}$  shifted 46.3 mV/ $\log[\text{H}^+]$ , close to the value of 58 mV/ $\log[\text{H}^+]$  expected for a proton-selective ion channel (fig. S8C). In response to hyperpolarizing voltage steps, OTOPI2 and OTOPI3 currents showed evidence of mild (OTOPI3) or no (OTOPI2) voltage dependence (fig. S8, B and D). When expressed in HEK-293 cells and assessed with microfluorimetry, both OTOPI2 and OTOPI3 conducted protons into the cell cytosol in response to lowering  $\text{pH}_o$  (fig. S10),

### Fig. 3. An evolutionarily conserved family of genes, expressed in diverse tissues and encoding proton channels.

(A) Maximum-likelihood phylogenetic tree from the multisequence alignment of 13 otopetrin domain proteins. Scale bar indicates amino acid substitutions per site. dm, *Drosophila melanogaster*; ce, *Caenorhabditis elegans*. (B) Distribution of *Otop* genes in selected murine tissues from microarray data (16). Scale represents expression level in arbitrary units (mean  $\pm$  SEM,  $n = 2$ ). (C, F, I) Representative traces ( $V_m = -80$  mV) showing currents evoked in *Xenopus* oocytes expressing OTOPI2, OTOPI3, or dmOTOPLc in response to varying pH<sub>o</sub> of the Na<sup>+</sup>-free extracellular solution. (D, G, J) *I*-*V* relationship (from voltage ramps at 1 V/s) from experiments as in (C), (F), and (I). (E, H, K) The average current induced at  $V_m = -80$  mV ( $\Delta I$ ) as a function of pH for oocytes expressing each of the channels (black circles; mean  $\pm$  SEM,  $n = 3$  to 7) and for uninjected oocytes (gray triangles; mean  $\pm$  SEM,  $n = 3$ ).



providing evidence that, like OTOPI, they form proton channels.

There are three genes in the genome of *Drosophila melanogaster* that encode proteins that appear to be evolutionarily related to mOTOP1 (12, 14) (Fig. 3A). The transcript CG42265 encodes dmOTOPLc, a protein of 1576 amino acids that over the region of similarity bears 14.1% amino acid identity with OTOPI. Despite the modest level of conservation, when expressed in *Xenopus* oocytes, dmOTOPLc conducted large currents in response to decreasing extracellular pH, indicating that it too forms a proton channel (Fig. 3, I to K). The shallow relation between the current amplitude and pH may endow the channel with a broader dynamic range.

OTOPI is required for the development of otoconia, calcium carbonate-based structures that sense gravity and acceleration in the vestibular system. Two mutations of *Otop1*, tilted (*tl*) and mergulhador (*mlh*; fig. S11A), lead to vestibular dysfunction in mice (14). These mutations affect trafficking of the protein to the cell surface in vestibular supporting cells (17). Mutant channels expressed in *Xenopus* oocytes produced smaller currents but otherwise had functional properties, such as sensitivity to Zn<sup>2+</sup> (fig. S11, B and C),

similar to those of wild-type OTOPI. This reduction in current magnitude may contribute to the vestibular dysfunction.

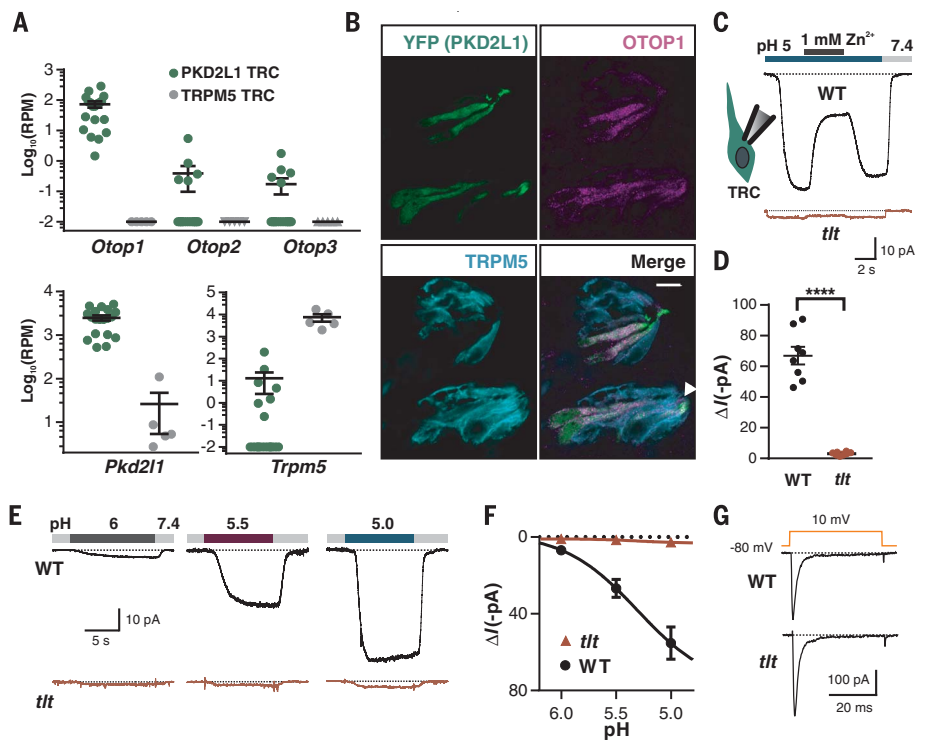
Finally, we sought to determine if OTOPI contributes to the proton current in acid-sensing taste receptor cells (10, 11). We confirmed that in single-cell transcriptome data, *Otop1* was expressed in PKD2L1 cells (19 out of 19) implicated in sour transduction (18), whereas *Otop2* and *Otop3* were expressed in much lower amounts, and none of the three *Otop* transcripts were detected in TRPM5 cells, which lack proton currents (Fig. 4A). By immunocytochemistry, we confirmed that OTOPI was present in taste cells in mouse circumvallate papillae that express *Pkd2l1* (Fig. 4B). To directly determine if OTOPI contributes to the proton current in taste cells, we measured currents in taste cells from either wild-type mice or mice that were homozygous for the *tl* mutation of *Otop1*. Mutation of *Otop1* resulted in significantly smaller proton currents than those measured in taste cells from wild-type mice (Fig. 4, C and D), over a range of H<sup>+</sup> concentrations (Fig. 4, E and F), indicating that OTOPI is a component of the proton channel in taste cells. Although the contribution of proton currents to acid-sensing or sour taste behavior

by mice is still speculative and complicated by contributions from multiple sensory organs and sensory receptors (19), the identification of OTOPI as forming a proton channel provides a tool with which to start dissecting this system.

Our data show that the *otopetrin* genes encode a family of ion channels that are unrelated structurally to previously identified ion channels and are highly selective for protons. Unlike Hv1, OTOPI is only weakly sensitive to voltage. Whether, like the viral proton channel M2 (13), low pH gates OTOPI is not clear. OTOPI channels conduct protons at normal resting potentials and can mediate the entry of protons into cells. Most cells guard against proton entry, which is generally cytotoxic. Thus, we expect that OTOPI channels are restricted to cell types that use changes in intracellular pH for cell signaling or to regulate biochemical or developmental processes. Along with a role in formation of vestibular otoconia (14), OTOPI has been shown to protect mice from obesity-induced metabolic dysfunction (15), and it is up-regulated in dorsal root ganglion cells in response to cell damage (20). The knowledge that this gene family encodes proton channels can be used to understand its contribution to physiology and disease.

**Fig. 4. Requirement of *Otop1* for the proton current in taste receptor cells.**

(A) Read counts per million (RPM) for the genes indicated from RNA-sequencing data obtained from single PKD2L1 ( $n = 19$ ) or TRPM5 taste cells ( $n = 5$ ). 0 RPM was adjusted to 0.01 RPM. (B) Confocal images showing taste buds in the circumvallate papillae from a mouse in which *Pkd2l1* drives expression of YFP, immunostained with antibodies against YFP (green), OTOPI1 (magenta), and TRPM5 (cyan). Scale bar, 10  $\mu$ M. Arrow indicates taste pore. (C) Current in response to a pH 5.0 stimulus in isolated PKD2L1 TRCs from *tlt* mutant or wild-type (WT) mice in NMDG<sup>+</sup>-based solution ( $V_m = -80$  mV). (D) Average data from experiments as in (C) (\*\*\*\* $P < 0.0001$  by two tailed  $t$  test,  $n = 8$  cells per genotype). (E) Response of PKD2L1 TRCs to NMDG<sup>+</sup>-based extracellular solution of varying pH ( $V_m = -80$  mV). (F) Average data from experiments as in (E). (G) Voltage-gated Na<sup>+</sup> currents in TRCs from *tlt* and wild-type mice were indistinguishable ( $P > 0.05$ , two-tailed  $t$  test).

**REFERENCES AND NOTES**

- B. Hille, *Ionic Channels of Excitable Membranes* (Sinauer, Sunderland, MA, 2001).
- W. A. Catterall, G. Wisedchaisri, N. Zheng, *Nat. Chem. Biol.* **13**, 455–463 (2017).
- E. Gouaux, R. Mackinnon, *Science* **310**, 1461–1465 (2005).
- T. E. Decoursey, *Physiol. Rev.* **83**, 475–579 (2003).
- L. H. Pinto, L. J. Holsinger, R. A. Lamb, *Cell* **69**, 517–528 (1992).
- T. E. Decoursey, *Biophys. J.* **60**, 1243–1253 (1991).
- I. S. Ramsey, M. M. Moran, J. A. Chong, D. E. Clapham, *Nature* **440**, 1213–1216 (2006).
- M. Sasaki, M. Takagi, Y. Okamura, *Science* **312**, 589–592 (2006).
- D. Morgan *et al.*, *Proc. Natl. Acad. Sci. U.S.A.* **106**, 18022–18027 (2009).
- R. B. Chang, H. Waters, E. R. Liman, *Proc. Natl. Acad. Sci. U.S.A.* **107**, 22320–22325 (2010).

- J. D. Bushman, W. Ye, E. R. Liman, *FASEB J.* **29**, 3014–3026 (2015).
- I. Hughes *et al.*, *BMC Evol. Biol.* **8**, 41 (2008).
- I. V. Chizhnikov *et al.*, *J. Physiol.* **494**, 329–336 (1996).
- B. Hurlle *et al.*, *Hum. Mol. Genet.* **12**, 777–789 (2003).
- G. X. Wang *et al.*, *Diabetes* **63**, 1340–1352 (2014).
- C. Wu *et al.*, *Genome Biol.* **10**, R130 (2009).
- E. Kim *et al.*, *Mol. Cell. Neurosci.* **46**, 655–661 (2011).
- A. L. Huang *et al.*, *Nature* **442**, 934–938 (2006).
- E. R. Liman, Y. V. Zhang, C. Montell, *Neuron* **81**, 984–1000 (2014).
- A. K. Reinhold *et al.*, *PLOS ONE* **10**, e0123342 (2015).

**ACKNOWLEDGMENTS**

E.R.L. and the University of Southern California have filed a provisional patent application no. 62/537,900 that claims methods of screening molecules that modulate Otopetrin-dependent ion channel activities. We thank S. Rao, L. Goggins, A. Bernanke, P. Uren, and members of the Nuzhdin lab for

technical assistance; J. Bushman for assistance with electrophysiology; and D. Arnold, B. Bean, B. Herring, and R. Kramer for careful reading of the manuscript. Funding was provided by the NIH grants R01DC013741 and R21DC012747 (to E.R.L.) and R01HG006015 (to A.D.S.).

**SUPPLEMENTARY MATERIALS**

www.sciencemag.org/content/359/6379/1047/suppl/DC1  
Materials and Methods  
Figs. S1 to S11  
Table S1  
References (21–34)

13 July 2017; accepted 8 January 2018  
Published online 25 January 2018  
10.1126/science.aao3264

## An evolutionarily conserved gene family encodes proton-selective ion channels

Yu-Hsiang Tu, Alexander J. Cooper, Bochuan Teng, Rui B. Chang, Daniel J. Artiga, Heather N. Turner, Eric M. Mulhall, Wenlei Ye, Andrew D. Smith and Emily R. Liman

*Science* **359** (6379), 1047-1050.

DOI: 10.1126/science.aao3264originally published online January 25, 2018

### The proton channel behind sour taste

Although many proteins that form ion channels in cell membranes have been described, none that selectively conduct protons into eukaryotic cells have been identified. Tu *et al.* used a genetic screen to pinpoint candidate genes that might encode such a protein from mouse taste receptor cells (see the Perspective by Montell). They identified the known protein otopetrin and showed that it conferred proton conductance when expressed in cultured human cells. Their results indicate that otopetrin may function in sensory recognition of sour (acidic) taste in humans and other organisms.

*Science*, this issue p. 1047; see also p. 991

#### ARTICLE TOOLS

<http://science.sciencemag.org/content/359/6379/1047>

#### SUPPLEMENTARY MATERIALS

<http://science.sciencemag.org/content/suppl/2018/01/24/science.aao3264.DC1>

#### RELATED CONTENT

<http://science.sciencemag.org/content/sci/359/6379/991.full>

#### REFERENCES

This article cites 33 articles, 8 of which you can access for free  
<http://science.sciencemag.org/content/359/6379/1047#BIBL>

#### PERMISSIONS

<http://www.sciencemag.org/help/reprints-and-permissions>

Use of this article is subject to the [Terms of Service](#)